PARTICLE-BEAM BEHAVIOR IN THE SNS LINAC WITH SIMULATED AND RECONSTRUCTED BEAMS*

S. Nath, J. Billen, J. Stovall, H. Takeda, and L. M.Young, LANL, Los Alamos, NM 87545, USA

K. Crandall, Tech Source, Santa Fe, NM, USA, and D. Jeon, SNS/ORNL, Oak Ridge, TN, USA

Abstract

The Spallation Neutron Source (SNS) project is a collaborative effort between Brookhaven, Argonne, Jefferson, Lawrence Berkeley, Los Alamos and Oak Ridge National Laboratories. Los Alamos has designed the entire linac for this accelerator complex. The final design of the SNS linac is comprised of both normal- and super-conducting RF (SRF) structures. The normal-conducting linac section up to 185 MeV, consists of a 2.5-MeV RFQ, a Medium Energy Beam Transfer (MEBT) line, a 402.5-MHz DTL, followed by a 805-MHz CCL. The SRF structure accelerates the beam from a nominal energy of 185 MeV to 1000 MeV. The SRF section consists of two, a medium beta (β= 0.61), and a high beta (β= 0.81) sections. The base-line design of the linac was done with a simulated beam at the input to the DTL. In this paper, we present the behavior of particle-beams originating at different locations upstream of the DTL. Input beams include a simulated beam at the input to the RFQ and a beam reconstructed from measurements.

INTRODUCTION

An earlier paper [1] describes the baseline design and anticipated beam performance of the SNS linac. It is designed to deliver 1.4 MW of circulating beam in the ring at 1 GeV with room for upgrade. The beam from the RFQ at 2.5 MeV goes through a MEBT-chopper section followed by a DTL. At ~87 MeV, the beam from the 402.5-MHz DTL enters the 805-MHz CCL. The major portion of the linac, which accelerates the beam to 1.0 GeV, is a 805-MHz SRF linac that follows the CCL structure. This linac is designed to eventually handle a peak current of 52 mA and deliver 2.65-MW of beam with a 6% duty factor. The current configuration, however, delivers 1.5- MW corresponding to peak beam-current of 38 mA.

In the baseline linac design phase, a simulated beam at the entry to the DTL (case 1) was used to evaluate the performance of the design. All through the changes of the base-line, including final change to the SRF structure for the high-energy portion of the linac, the design was evaluated with this simulated beam. In the next step of the design process, MEBT was included in the evaluation of the beam behavior. The simulated beam started at the beginning of the MEBT section after the RFQ (case2). The MEBT is a transport section where a second and final chopping [2] is performed. Due to constraints imposed by required beam profile in the chopping section, the MEBT design was revisited several times. Finally, it was reconfigured to add slits removing the halo produced in this section and to match the beam to the input to the DTL. This modified MEBT is used for case 3 where simulations are done with a 4-D waterbag distribution at the input to the RFQ. Incidentally, loss and error simulations [3] in the normal conducting section of the linac were done with beam-collimators in the MEBT.

Finally, in case 4, we studied the performance of the linac with beam that was reconstructed from the beam measurement at the end of the LEBT and then transported through the RFQ and the modified MEBT. In the next sections, we present the results for all the four cases. No errors were included in any of the simulations. Beam dynamics code, LINAC was used for all simulation runs.

SIMULATION

Modified MEBT

It was recognized very early in the simulation studies that significant halo develops while the beam passes through the MEBT. Some of the halo particles survive through most of the normal conducting linac but get lost primarily near the end of the CCL section. Studies were conducted to mitigate this problem; the MEBT was modified; horizontal (both +x and -x) scrappers were added, in addition to the vertical +y beam chopper target that nominally intercepts and removes 1% of the beam. Details on this modification are reported in an accompanying paper [4].

Matching Through MEBT

The rms-ellipse parameters and emittances at the input to the MEBT were calculated from the case 3 distribution after filtering out the low energy stragglers i.e., looking at the output beam from the RFQ with a simulated 4-D waterbag input. A 6-D waterbag distribution having the same rms properties was generated and was transported to the third buncher cavity in the MEBT. TRACE was used for adjusting the two quads upstream of this buncher cavity to produce a round beam at this cavity. The beam was then transmitted to the beginning of the DTL to get the emittances at the entrance to the DTL. Again TRACE was used to find the match for the beam with these emittances at 38 mA. Finally, the third and fourth cavity and the four quads just upstream of the DTL were adjusted (by using TRACE) to match the beam from the MEBT to the DTL.

Simulation Procedure

In case 1, a 6-D waterbag distribution of 100,000 particles was generated for the matched input to the DTL and run through the linac. For case 2, the simulated beam (6-D waterbag distribution) starts at the beginning of the

MEBT i.e., at the output point of the RFQ. For case 3, we use a simulated 4-D waterbag distribution of 100,000 particles representing 40 mA at the input to the RFQ. The output at the RFQ contains ~0.5% of low energy particles not accelerated by the RFQ. After filtering out the low energy particles the current reduces to ~37.2 mA, somewhat less than 38 mA used for cases 1 and 2. No attempt is made to adjust the MEBT to rematch the beam into the DTL.
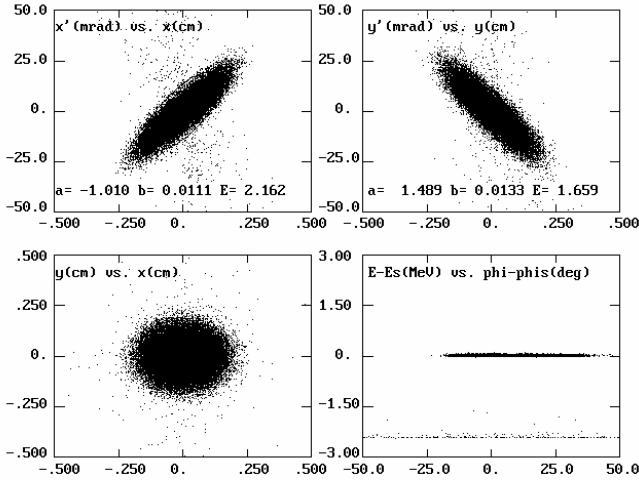

Figure 1. Phase-space plots at the RFQ output for case 4 showing the low energy particles from the RFQ.
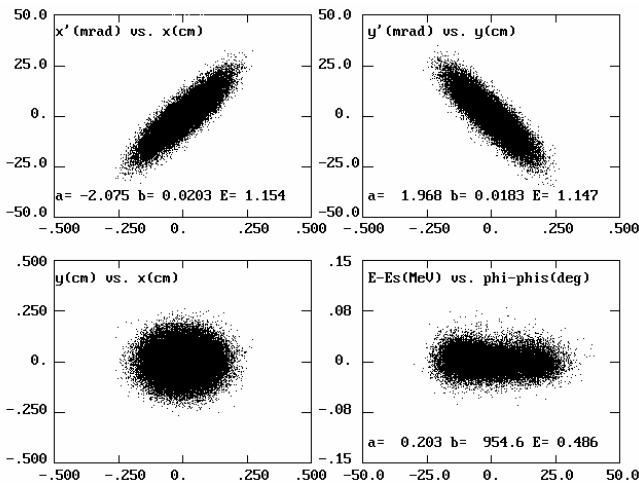

Figure 2. Phase-space plots at the RFQ output for case 4 after filtering out the low energy particles.

For case 4, we start with an initial particle distribution derived from x and y beam emittance measurements [5] made at slightly different longitudinal locations. We transform to the midpoint between the measurements without space charge and construct a numerical particle distribution. This particle distribution continues backward through the LEBT to a reference point upstream of the deflection electrodes. The computer code PARMELA, is used to verify that forward and backward beam transport with 3-D space charge is completely reversible. For our beam simulation studies, we transport the beam starting at

this reference point and go through the 3-D fields of the LEBT. A description of the generation of distribution and transport through the LEBT is described in detail in [5].

Figures 1 and 2 show the phase space distributions at the RFQ output point before and after the removal of the low energy particles that made through the RFQ without acceleration. After removal of low energy particles, the beam current reduces to 36.4 mA. As in case 3, no attempt was made to rematch the beam into the DTL. This input distribution should be compared to the simulated input distribution of case 2 shown in Figure 3.
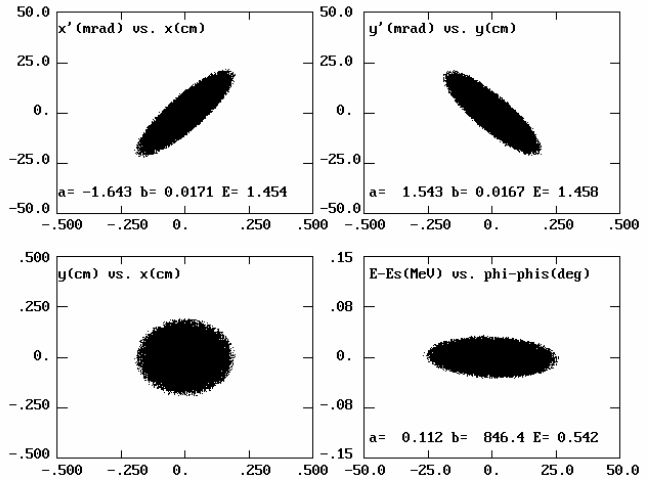

Figure 3. Phase-space plots of the simulated 6-D waterbag distribution at the input to the MEBT for case 2.

RESULTS

Figure 4 shows the normalized rms x- and y-emittance along the length of the entire linac for all the four cases. As can be seen from the plots, for cases 1 and 2, there is virtually no emittance growth in either x or y emittance. The same is true for longitudinal emittance (not shown).
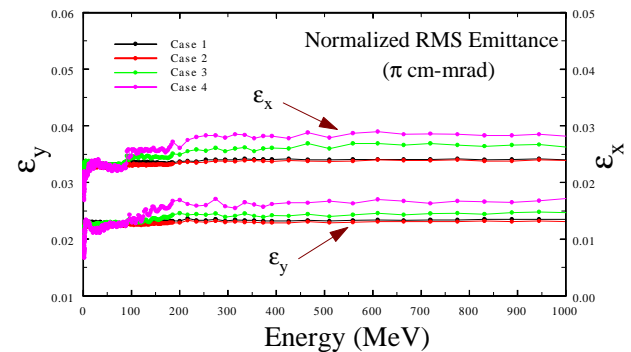

Figure 4. Normalized, rms x- and y-emittance along the length of the linac for four different cases.

Since no attempt is made to adjust the MEBT to rematch the beam coming out of the RFQ for cases 3 and 4, the beam emittance shows growth at the DTL and CCL junctions. Furthermore, there is gradual increase in transverse emittances along the CCL. This is understandable as transverse focusing is gradually

reduced along the CCL to make a smooth transition in focusing strength to the weaker focusing in the SRF section due to longer periodic lattice of the SRF lattice.
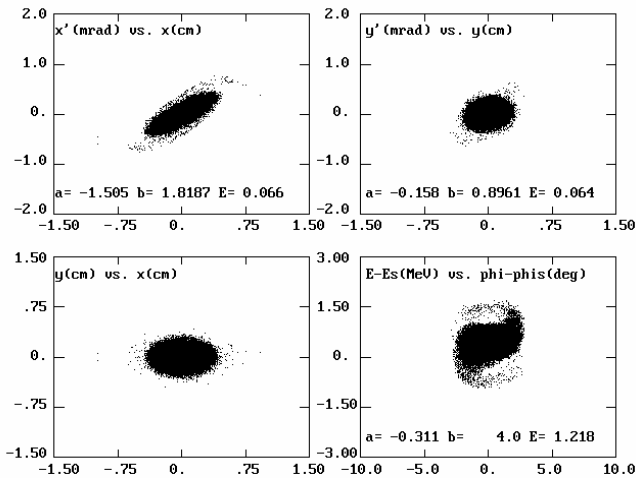

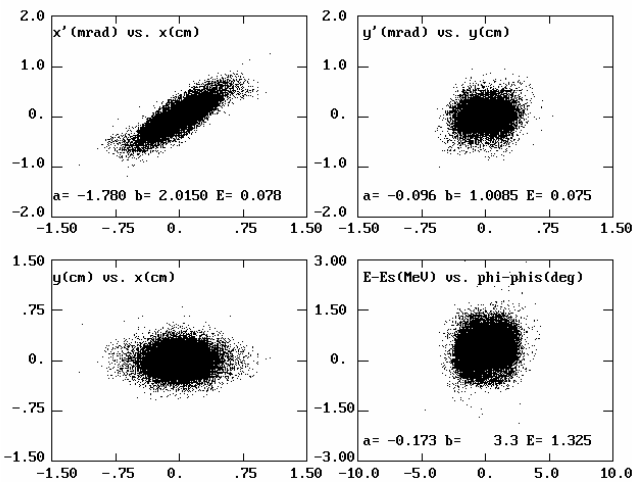Figure 5. Phase-space projections at the end of the linac for case 2.

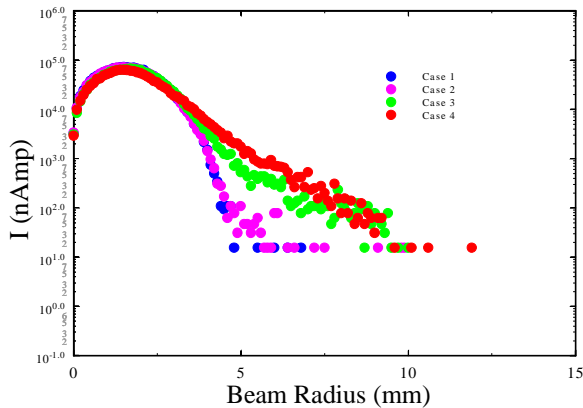Figure 6. Phase-space projections at the end of the linac for case 4.

Figure 7. Radial-distribution of particles at the end of the linac for all four cases.

Figures 5 and 6 show phase space projections at the end of the linac (1 GeV) for cases 2 and 4 respectively. As expected, there is considerable growth in the transverse beam extent in case 4 compared to case 2. In addition, there is some halo formation. This is more clearly visible in Figure 7 where the radial distribution of the particles at the linac-end is shown for all four cases. While for cases 1 and 2, the beam virtually does not extend beyond ~5 mm (within statistics), the beam extends to ~10 mm for cases 3 and 4. Also, the beam distributions are more diffused in cases 3 and 4 indicative of halo in the beam.

Finally, the radial dimensions of the beam, both rms as well as 99% beam-size, along the entire length of the linac are shown in Figure 8. Predictably, the beam size gradually increases from the DTL towards the end of the CCL as the transverse focusing slowly decreases in that portion of the linac.
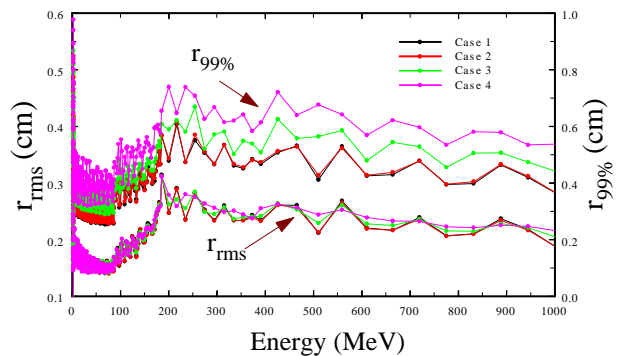

Figure 8. Radial beam-size, both rms and 99% along the length of the linac.

SUMMARY

The MEBT was tuned for a peak current of 38 mA and specific values of transverse and longitudinal emittances. In the examples discussed above, no attempt was made to rematch the beam out of the RFQ to the input of the DTL. Therefore, some mismatch is present in the beam coming out of the RFQ. This would be the case in reality if no dedicated online beam-measurement devices are present at the input to the DTL. In this context, the simulations with beam from the RFQ without rematching the MEBT are representative of realistic operational scenarios.

REFERENCES

[1] J. Stovall et al., "Expected Beam Performance of the SNS Linac," Proceedings of the 2001 Particle Accelerator Conference, p 446, June 18-22, 2001, Chicago, IL, USA.

[2] J. Staples et al., "The SNS Front-end Accelerator Systems," Proceedings of the XIX International Linac Conference, 1998, Chicago, IL, USA.

[3] S. Nath et al., ASAC presentation, October 2001, SNS/ORNL, Tenn., USA.

[4] D. Jeon et al., invited paper to this conference.

[5] S. Nath et al., Proceedings of the XXI International Linac Conference, p 319, 2002, Gyongju, S. Korea.